

RESEARCH

Open Access



GR113808, a serotonin receptor 4 antagonist, prevents high-fat-diet-induced obesity, fatty liver formation, and insulin resistance in C57BL/6J mice

Min Hee Kim^{1,2}, Su-Jeong Kim², Woo-Jae Park^{3*}, Dae Ho Lee⁴ and Kyoung-Kon Kim^{5*}

Abstract

Background The burden of nonalcoholic fatty liver disease is increasing, and limited therapeutic drugs are available for its treatment. Serotonin binds to approximately 14 serotonin receptors (HTR) and plays diverse roles in obesity and metabolic complications. In this study, we focused on the function of HTR4 on nonalcoholic fatty liver disease using GR113808, a selective HTR4 antagonist.

Methods Male C57BL/6J mice were fed high-fat diet for 12 weeks with intraperitoneal GR113808 injection, and HTR expression, weight changes, glucose and lipid metabolism, hepatic fat accumulation, changes in adipose tissue, the changes in transcriptional factors of signaling pathways, and inflammations were assessed. Hep3B cells and 3T3-L1 cells were treated with siRNA targeting HTR4 to downregulate its expression and then cultured with palmitate to mimic a high-fat diet. The changes in transcriptional factors of signaling pathways, and inflammations were assessed in those cells.

Results After feeding a high-fat diet to male C57BL/6J mice, HTR4 expression in the liver and adipose tissues decreased. GR113808 suppressed body weight gain and improved glucose intolerance. Furthermore, GR113808 not only decreased fatty liver formation but also reduced adipose tissue size. Additionally, GR113808 reduced inflammatory cytokine serum levels and inflammasome complex formation in both tissues. Palmitate treatment in HTR4-downregulated Hep3B cells, also reduced peroxisome proliferator-activated receptor γ and sterol regulatory element-binding protein-1 pathway induction as well as inflammasome complex formation, thus decreasing inflammatory cytokine levels. HTR4 downregulation in 3T3-L1 cells also reduced palmitate-induced inflammasome complex formation and inflammatory cytokine production. Palmitate-induced insulin resistance in Hep3B cells, but not in 3T3-L1 cells, was improved by HTR4 downregulation.

*Correspondence:

Woo-Jae Park
ooze@cau.ac.kr
Kyoung-Kon Kim
zaduplum@aim.com

Full list of author information is available at the end of the article



© The Author(s) 2024. **Open Access** This article is licensed under a Creative Commons Attribution-NonCommercial-NoDerivatives 4.0 International License, which permits any non-commercial use, sharing, distribution and reproduction in any medium or format, as long as you give appropriate credit to the original author(s) and the source, provide a link to the Creative Commons licence, and indicate if you modified the licensed material. You do not have permission under this licence to share adapted material derived from this article or parts of it. The images or other third party material in this article are included in the article's Creative Commons licence, unless indicated otherwise in a credit line to the material. If material is not included in the article's Creative Commons licence and your intended use is not permitted by statutory regulation or exceeds the permitted use, you will need to obtain permission directly from the copyright holder. To view a copy of this licence, visit <http://creativecommons.org/licenses/by-nc-nd/4.0/>.

Conclusions In summary, GR113808 protected against fatty liver formation and improved inflammation in the liver and adipose tissue. Downregulation of HTR4 ameliorated insulin resistance in the liver. These results suggest that HTR4 could serve as a promising therapeutic target for metabolic diseases.

Keywords Serotonin receptor 4, Insulin resistance, Fatty liver, Inflammation, Obesity

Introduction

Currently, the most common chronic liver disease is nonalcoholic fatty liver disease (NAFLD), with a global prevalence of approximately 25% in the adult population, and it has become the leading cause of end-stage liver disease [1, 2]. NAFLD is defined as the presence of steatosis in >5% of hepatocytes and includes two distinct conditions: (1) nonalcoholic fatty liver and steatosis with or without mild lobular inflammation and (2) nonalcoholic steatohepatitis and steatosis with fibrosis, cirrhosis, or hepatocellular carcinoma [3]. NAFLD is associated with metabolic risk factors, especially obesity and type 2 diabetes, and has been designated as a metabolic dysfunction-associated fatty liver disease by some experts because of its association with cardiometabolic risk factors [1]. Although less than 10% of patients with NAFLD have complications of end-stage liver disease in the form of cirrhosis or hepatocellular carcinoma, the absolute number of patients with end-stage liver disease due to NAFLD is considerable owing to its high prevalence, and the disease burden of NAFLD is increasing [1]. Although pioglitazone and vitamin E are suggested drugs for biopsy-proven nonalcoholic steatohepatitis, there is no approved pharmacotherapy for the direct treatment of NAFLD [3].

First reported in the 1940s, serotonin (5-hydroxytryptamine, 5-HT) is a monoamine with various biological effects in both the central nervous system and peripheral tissues. 5-HT can bind to at least 14 different 5-HT receptors, of which there are seven classes (5-hydroxytryptamine receptors; HTR1–7). Most of these are G-protein-coupled receptors, with the exception of HTR3 which is a ligand-gated ion channel [4]. In the central nervous system, 5-HT acts as a neurotransmitter and modulates human behavioral and neuropsychological processes; however, it is also involved in vascular biology, cardiac function, respiration, digestion, pain perception, ejaculation, and reproductive function in peripheral tissues. Because 5-HT participates in the regulation of food intake in the central nervous system, some 5-HT-related drugs, such as fenfluramine, sibutramine, and lorcaserin, have been used to suppress appetite [5]. Moreover, in the periphery, 5-HT plays a role in insulin secretion [6], liver regeneration [7], and inflammatory processes [8].

Several pathophysiological steps can be targeted by pharmacotherapy to improve NAFLD and prevent its progression, including hepatic fat accumulation, oxidative stress, endoplasmic reticulum (ER) stress,

inflammation, apoptosis, and hepatic fibrosis [2]. Considering the biological effects of 5-HT on appetite control, insulin secretion, liver regeneration, and inflammation, it may be a potential solution for NAFLD. However, as mentioned above, many types of receptors with different biological effects have already been discovered, and little is known about which receptors are appropriate targets for NAFLD therapy.

Methods

Aim

In this study, we sought to determine the appropriate HTR for NAFLD treatment and examined the metabolic effects and underlying mechanisms of molecules related to the receptor.

As described in the results, we focused on the role of HTR4 among various HTR in NAFLD in this study. Therefore, we investigated the metabolic effects and mechanisms of GR113808, a known HTR4 antagonist, in an HFD-induced NAFLD model. C57BL/6J mice were fed high-fat diet (HFD) for 12 weeks with intraperitoneal GR113808 injection, and HTR expression, weight changes, glucose and lipid metabolism, hepatic fat accumulation, the changes in adipose tissue, the changes in transcriptional factors of signaling pathways, and inflammations were assessed. Hep3B cells and 3T3-L1 cells were treated with HTR4 siRNA and cultured with palmitate to mimic a HFD. The changes of transcriptional factors of signaling pathways, and inflammations were assessed in those cells.

Animals and the glucose tolerance test (GTT)

NAFLD and type 2 diabetes mellitus are induced by feeding mice a high-fat diet for 12 weeks [9], and long-term (24–25 weeks) HFD feeding can induce liver fibrosis in mice [10]. Therefore, mice fed with an HFD resemble a human obesity model.

Six-week-old male C57BL/6J mice were purchased from Orient Bio (Seongnam, Korea) and housed in a specific pathogen-free environment. Following a 1-week acclimation period, the mice were freely fed either an HFD, (D12492, Research diet) (60% fat, 20% carbohydrate, and 20% protein; 21.92 kJ/g) or a standard chow diet (SCD, D12450K) (10% fat, 70% carbohydrate, and 20% protein; 16.11 kJ/g) for 12 weeks with intraperitoneal GR113808 injection (1 mg/kg/week) (10 mice each; 10 mice used for the GTT [11]). GR113808 was dissolved in dimethyl sulfoxide at a concentration of 20 mg/

ml and stored at -20°C . It was then diluted with sterile phosphate-buffered saline (PBS) (1:100) and injected into mice. Mice were injected with GR113808 three times a week in the morning (10 AM). Control mice received the same amounts of vehicle injections. Body weight was measured weekly. During the experiments, food intake was measured every 12 h by manually weighing the food in the individual cages. At the end of this experiment, the weight change, glucose and triglyceride metabolism, hepatic fat accumulation, and the change in adipose tissue were recorded to investigate the metabolic effects of HTR4 on NAFLD.

After 12 weeks of feeding, a GTT was performed as previously described [12]. After 18 h of starvation, mice were intraperitoneally injected with glucose (2.0 g/kg), and blood glucose levels were measured at 0 (before injection), 15, 30, 45, 60, 90, and 120 min using an automatic glucometer (ACCU-CHEK PERFORMA, Roche Diagnostics, Germany). After the GTT experiment, the mice were anesthetized by placing them in a closed chamber and ventilating with 2% isoflurane in oxygen for approximately 2–3 min. Under deep anesthesia with isoflurane, the mice were euthanized using a high concentration of CO_2 [13]. After confirmation of apnea, the sera, livers, and adipose tissues were isolated, weighed, and stored at -80°C for further analyses.

Cell culture, siRNA transfection, and insulin treatment

Hep3B cells and 3T3-L1 cells were cultured in Dulbecco's Modified Eagle Medium supplemented with 10% fetal bovine serum and 1% penicillin/streptomycin. siHTR4 (human: 144644, mouse: 158191) was purchased from Thermo Fisher Scientific Inc. (Waltham, MA, USA) and transfected using Lipofectamine RNAiMAX Transfection Reagent (Invitrogen, Carlsbad, CA, USA) following the manufacturer's protocol. In some experiments, cells were transfected with siHTR4, followed by treatment with 200 μM palmitate for 18 h. Subsequently, cells were treated with 1 nM insulin. After 2 or 5 min of insulin treatment, the cells were promptly frozen by immersion in liquid nitrogen and lysed using radioimmunoprecipitation assay (RIPA) buffer.

Materials

The following materials were purchased as indicated: (1) anti- α -tubulin antibody and insulin from Sigma-Aldrich (St. Louis, MO, USA); (2) anti-phospho-PERK (protein kinase R-like endoplasmic reticulum kinase), anti-phospho-eIF2 α (eukaryotic translation initiation factor 2 α), anti-PPAR- γ (peroxisome proliferator-activated receptor γ), anti-CD36 (cluster of differentiation 36), anti-NLRP3 (NOD-like receptor family pyrin domain containing 3), anti-FAS (fatty acid synthase), anti-SCD-1 (stearoyl-CoA desaturase-1), anti-Akt, and

anti-phospho-Akt antibodies from Cell Signaling Technology (Beverly, MA, USA); (3) anti-HTR4 antibody from Abcam (Cambridge, MA, USA); (4) interleukin (IL) 1 β antibody from Novus Biologicals (Littleton, CO, USA); (5) anti-ASC (apoptosis-associated speck-like protein containing a caspase-recruitment domain) and anti-caspase-1 antibodies from Santa Cruz Biotechnology (Santa Cruz, CA, USA); (6) GR113808 from Tocris Bioscience (Bristol, UK); (7) anti-mouse-HRP (horseradish peroxidase, 115-036-003) and anti-rabbit-HRP (111-035-003) antibodies from the Jackson Laboratory (Bar Harbor, ME, USA).

Enzyme-linked immunosorbent assay (ELISA)

The tumor necrosis factor (TNF)- α , IL-1 β , and IL-6 levels in the serum and media were measured using ELISA kits (TNF- α , IL-1 β , and IL-6 Human and Mouse ELISA kits, Komabiotek, Seoul, Korea) according to the manufacturer's instructions. Serum adiponectin levels were measured using a Mouse Adiponectin/Acrp30 Quantikine ELISA Kit (R&D Systems, Minneapolis, MN, USA).

Western blotting

Tissues, Hep3B cells, and 3T3-L1 cells were homogenized in RIPA buffer (50 mM Tris-HCl [pH 7.5], 150 mM NaCl, 1% Nonidet P-40, 0.5% sodium deoxycholate, and 0.1% sodium dodecyl sulfate [SDS]) with protease and phosphatase inhibitors (Sigma-Aldrich) and incubated on ice for 30 min. After centrifugation (10,000 \times g, 10 min, 4 $^{\circ}\text{C}$), the protein levels in the supernatants were examined, and 50 μg of protein was separated on 8–15% SDS polyacrylamide gels before being transferred to nitrocellulose membranes (Bio-Rad Laboratories, Hercules, CA, USA). The membranes were blocked using 5% bovine serum albumin (Sigma-Aldrich) in TBST (TBS with 0.1% Tween-20) for 1 h and sequentially incubated with primary (1:1000 dilutions) and secondary (1:10,000 dilutions) antibodies. Protein bands were detected using EzWestLumi Plus Reagents (ATTO Corporation, Tokyo, Japan) on a Chemidoc MP imaging system (Bio-Rad Laboratories). The densitometric analyses of western blots were conducted using ImageJ software (version 1.51; <http://imagej.net>; National Institutes of Health, Bethesda, MA, USA).

Hematoxylin and eosin staining

The mouse livers and adipose tissues were fixed in a 4% paraformaldehyde solution overnight and embedded in paraffin blocks. Tissue sections were cut at 4 μm and stained with hematoxylin and eosin. Two adipocytes were randomly selected from each image, and their diameters were measured using ImageJ software.

Real-time PCR

Total mRNA was extracted from the livers and adipose tissues using NucleSpin RNA (Macherey-Nagel, Germany) or an RNeasy Lipid Kit (Qiagen, Valencia, CA, USA), and cDNA was synthesized using ReverTra Ace qPCR RT Master Mix (Toyobo, Japan). qPCR was performed using Thunderbird SYBR qPCR mix (Toyobo) on a Bio-Rad CFX96 System (Bio-Rad). The temperature was initially held for 1 min at 95 °C, and then 40 cycles comprising 15 seconds at 95 °C followed by 45 seconds at 60 °C were performed. Relative gene expression was calculated using the $2^{-\Delta\Delta C_t}$ method [14]. The primers used are listed in the Table S1.

Cholesterol, triglyceride, and high-density lipoprotein (HDL) and low-density lipoprotein (LDL) cholesterol measurements

Serum cholesterol, triglyceride, and HDL and LDL cholesterol levels were measured using the Reflotron System (Roche Diagnostics). The liver triglyceride levels were measured using a total triglyceride colorimetric assay kit (Biovision, Mountain View, CA, USA).

Statistical analyses

All experiments were repeated independently in triplicate, and the data are expressed as the mean \pm standard deviation (SD). Statistical significance was calculated using two-way ANOVA and a Tukey post hoc test for the GTT and body weight changes, and a two-sample student's *t*-test (R software v4.3.3, Vienna, Austria. <https://www.R-project.org/>, ggpubr v0.6.0) was used for other studies, with statistical significance set at $p < 0.05$. Among the four groups, including control (SCD), GR113808, HFD, and HFD+GR113808, comparisons of two groups were performed for the following pairs: (1) control vs GR113808, (2) control vs HFD, and (3) HFD vs HFD+GR113808.

Results

Selection of HTR subtype for the therapeutic target in NAFLD

We examined HTR expression in the liver and white adipose tissue (WAT) of HFD-fed mice to identify a candidate class of HTRs. The HFD increased HTR2a expression in the liver but decreased HTR4 and HTR6 expression (Fig. 1A). Additionally, HTR2c, HTR3a, HTR4, HTR5b, and HTR7 expression in WAT was reduced by HFD feeding (Fig. 1B). The expression of other HTRs (not shown in Fig. 1A and B) was not detected because of their low expression levels. We found that the HTR4 mRNA level was reduced in both the liver and WAT of HFD-fed mice. The HTR4 protein levels in the liver and WAT were examined and found to be reduced, similar to the HTR4 mRNA levels (Fig. 1C).

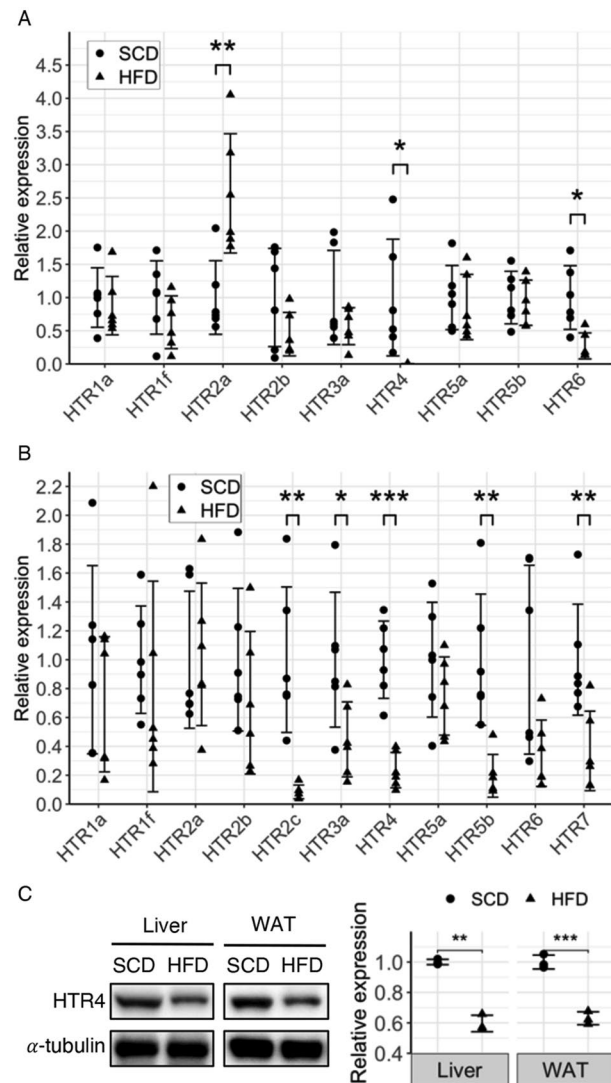


Fig. 1 HFD feeding reduces HTR4 expression in the liver and adipose tissues. C57BL/6 mice were fed an HFD for 12 weeks, and relative mRNA levels of HTR are analyzed in the liver (A) and WAT (B) ($n = 6$). (C) Representative western blots (left) and densitometric analysis (right) of HTR4 expression ($n = 3$) in the liver and WAT after 12 weeks of HFD feeding. A student's *t*-test was performed. Error bars on plots represent standard deviation (SD); * $p < 0.05$, ** $p < 0.01$, *** $p < 0.001$. Abbreviations HFD high-fat diet, HTR serotonin receptor, SCD standard chow diet, WAT white adipose tissue

Based on these results, we examined the role of HTR4 using HFD-fed mice.

The HTR4 antagonist GR113808 reduced HFD-induced body weight gain and improved glucose and triglyceride metabolism

To examine the role of HTR4 in body weight gain and fat accumulation in the liver, mice were fed an HFD and injected with GR113808, an HTR4 antagonist, for 12 weeks. First, we assessed food intake and found that GR113808 had no effect, indicating that HTR4

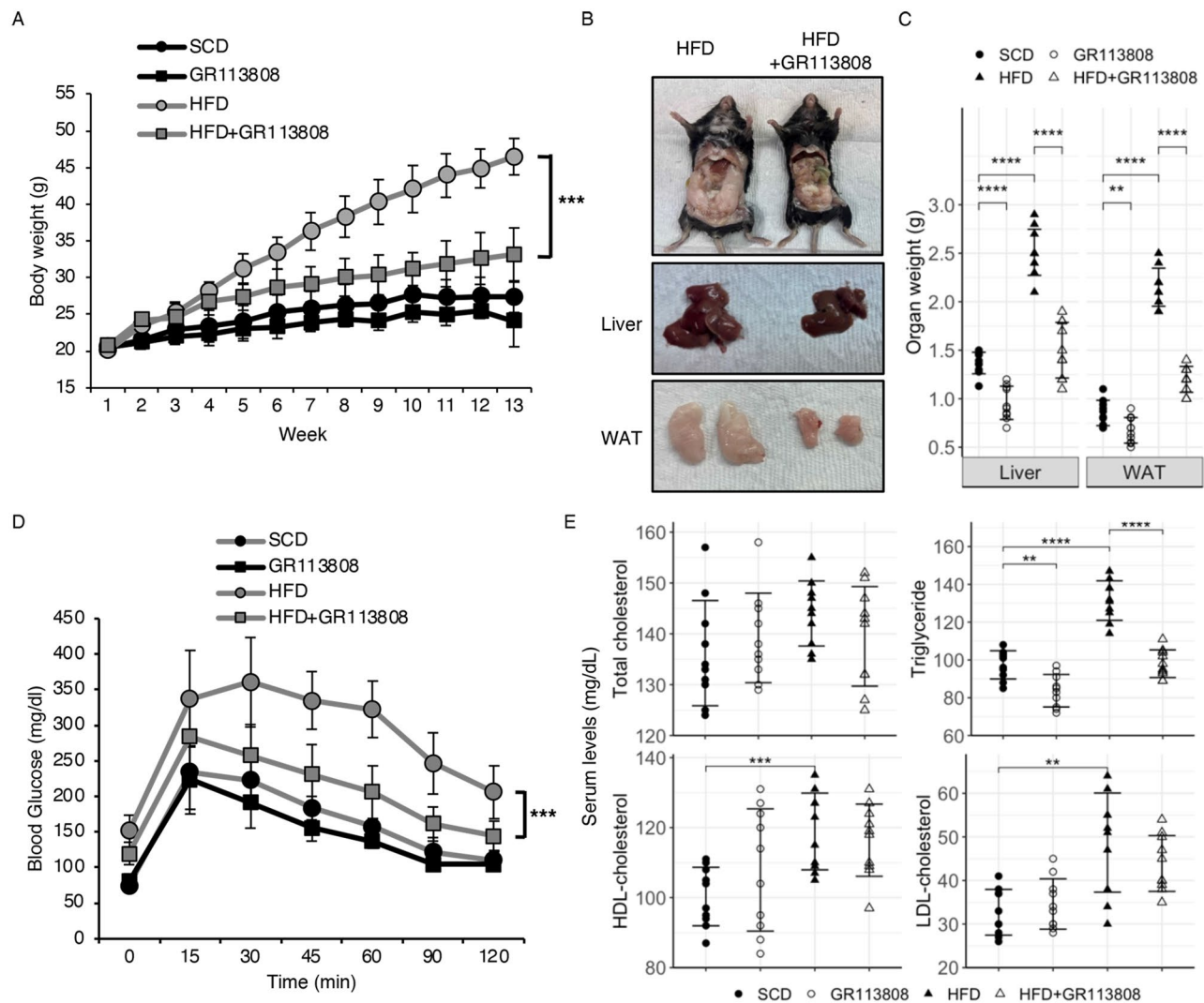


Fig. 2 GR113808 prevents HFD-induced body weight gain and insulin resistance. C57BL/6 mice were fed an HFD and treated with GR113808 (1 mg/kg/week) for 12 weeks. **(A)** Body weight gain during 12 weeks of HFD feeding with GR113808 treatment ($n=10$). The gross anatomical view of the morphology **(B)** and the organ weight ($n=10$) **(C)** of the liver and inguinal WAT after 12 weeks of HFD feeding are shown. **(D)** Glucose tolerance test after 12 weeks of HFD feeding ($n=10$). **(E)** Serum TG, cholesterol, and HDL and LDL cholesterol from mice fed the HFD ($n=10$). Two-way ANOVA and Tukey's post hoc test were performed for **(A, D)**; Student's *t*-test was performed for **(C, E)**. Error bars on plots represent standard deviation (SD); ** $p < 0.01$, *** $p < 0.001$, **** $p < 0.0001$. Abbreviations HDL high-density lipoprotein, HFD high-fat diet, LDL low-density lipoprotein, SCD standard chow diet, TG triglyceride, WAT white adipose tissue

antagonists did not affect appetite (Fig. S1). Additionally, GR113808 not only reduced body weight gain during HFD feeding (Fig. 2A) but also decreased weight gain of the liver and adipose tissues (Fig. 2B and C). Moreover, GR113808 improved postprandial glucose levels (Fig. 2D) and decreased serum triglyceride levels but did not affect cholesterol, HDL cholesterol, and LDL cholesterol levels (Fig. 2E).

GR113808 suppressed hepatic fat accumulation, via a transcriptional factor change, in mice fed an HFD

Next, we analyzed the histological appearance of the liver, which showed reduced fatty liver formation

following GR113808 injection (Fig. 3A). GR113808 injection also reduced hepatic triglyceride levels (Fig. 3B). To further understand this mechanism, we analyzed various signaling pathways. GR113808 decreased not only sterol regulatory element-binding protein 1c (SREBP-1c), FAS, SCD-1, and monoacylglycerol O-acyltransferase 1 (Mogat1), but also reduced PPAR- γ , CD36, and fatty acid binding protein 1 (FABP1) expression (Fig. 3C and D); these genes play critical roles in lipogenesis and fatty acid uptake [15, 16]. Additionally, GR113808 injection increased carnitine palmitoyl transferase 1a (Cpt1a) and PPAR- α expression in HFD-fed livers, but it did not affect gene expression of fatty acid transport protein 5 (FATP5)

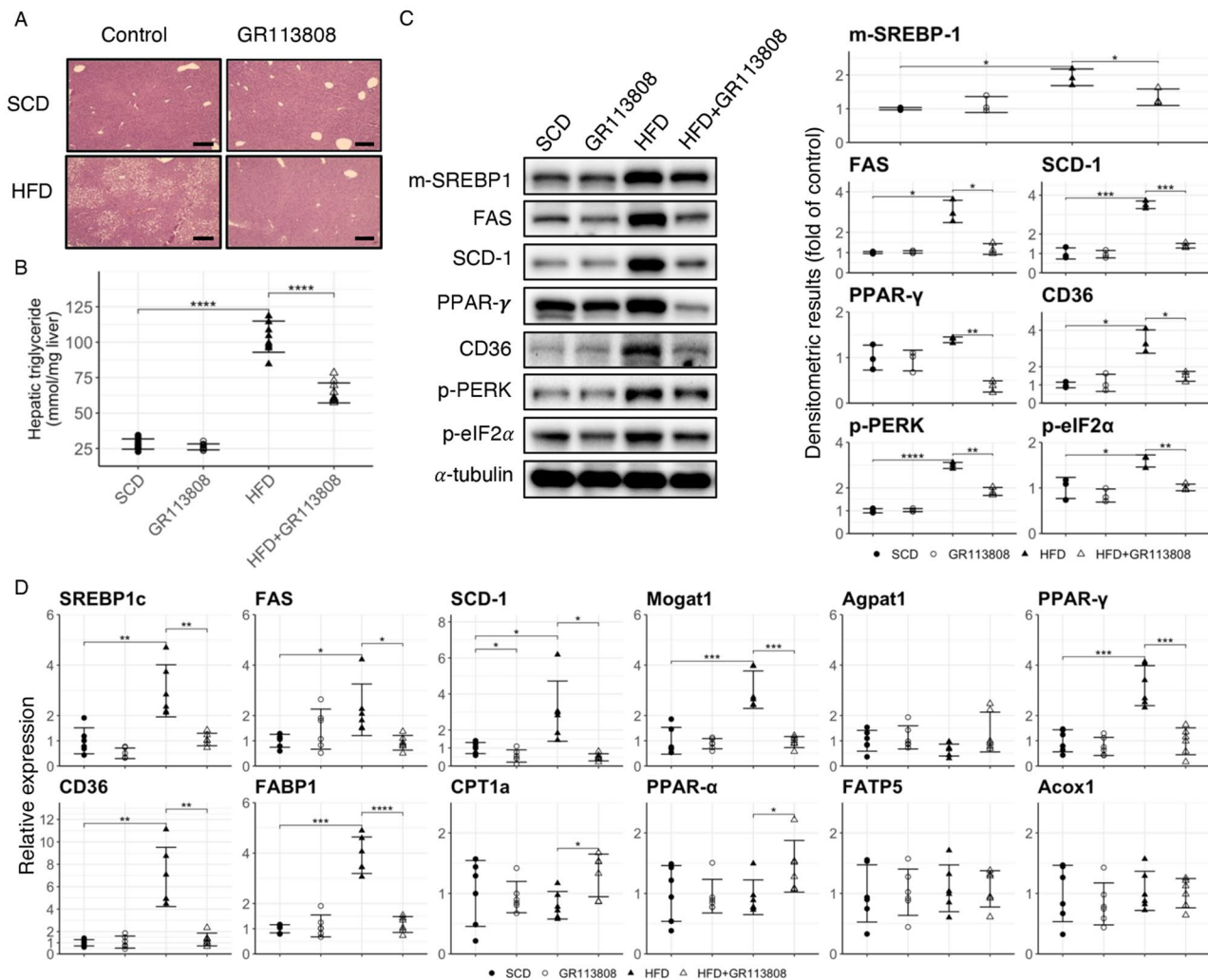


Fig. 3 GR113808 prevents HFD-induced fatty liver formation. **A** histological analysis of the liver (scale bar: 100 μ m) (**A**) and the triglyceride amount in (**B**) the liver ($n = 10$) are shown. (**C**) Representative western blots (left) and densitometric analysis (right) for the indicated antibody using liver lysates ($n = 3$). (**D**) Relative mRNA levels of genes related to lipogenesis (SREBP1c, FAS, SCD-1, Agpat1, PPAR- γ , and Mogat1), fatty acid uptake (CD36, FABP1, and FATP5), and fatty acid oxidation (CPT1a, Acox1, and PPAR α) in the livers of mice injected with GR113808 ($n = 6$). A student's *t*-test was performed. Error bars on plots represent standard deviation (SD); * $p < 0.05$, ** $p < 0.01$, *** $p < 0.001$, **** $p < 0.0001$. Abbreviations Acox1 acyl-CoA oxidase 1, Agpat1 1-acylglycerol-3-phosphate O-acyltransferase 1, CD36 cluster of differentiation 36, CPT1a carnitine palmitoyl transferase 1a, eIF2 α eukaryotic translation initiation factor 2 α , FABP fatty acid binding protein, FAS fatty acid synthase, FATP fatty acid transport protein, HFD high-fat diet, Mogat1 monoacylglycerol O-acyltransferase 1, PERK protein kinase R-like endoplasmic reticulum kinase, PPAR peroxisome proliferator-activated receptor, SCD standard chow diet, SCD-1 stearoyl-CoA desaturase 1, m-SREBP1 mature form of sterol regulatory element-binding protein 1

and acyl-CoA oxidase 1 (Acox1) (Fig. 3D). GR113808 also reduced PERK and eIF2 α phosphorylation (Fig. 3C), thus it decreased ER stress.

GR113808 reduced the size of adipocytes upon HFD feeding

HFD feeding increased the size of lipid droplets, but GR113808 prevented this increase in WAT droplet size (Fig. 4A and C). GR113808 reduced both the distribution of adipocyte size and mean adipocyte size in WAT under HFD conditions (Fig. 4C). Interestingly, GR113808 injection increased serum adiponectin and adiponectin

mRNA levels in adipose tissue under both SCD and HFD conditions (Fig. 4B and D). However, GR113808 did not affect the expression of genes involved in triglyceride synthesis (Mogat1, diacylglycerol O-acyltransferase 1 (Dgat1), and Dgat2), fatty acid synthesis (SCD-1), and fatty acid uptake (PPAR- γ and CD36) or peroxisome proliferator-activated receptor gamma coactivator 1-alpha (PGC1 α) (Fig. 4D). GR113808 decreased FAS expression and increased cell death-inducing DFFA-like effector A (Cidea), acetyl-CoA carboxylase alpha (ACACA), hormone-sensitive lipase (HSL), and adipose triglyceride lipase (Atgl) expression in WAT of HFD-fed mice and

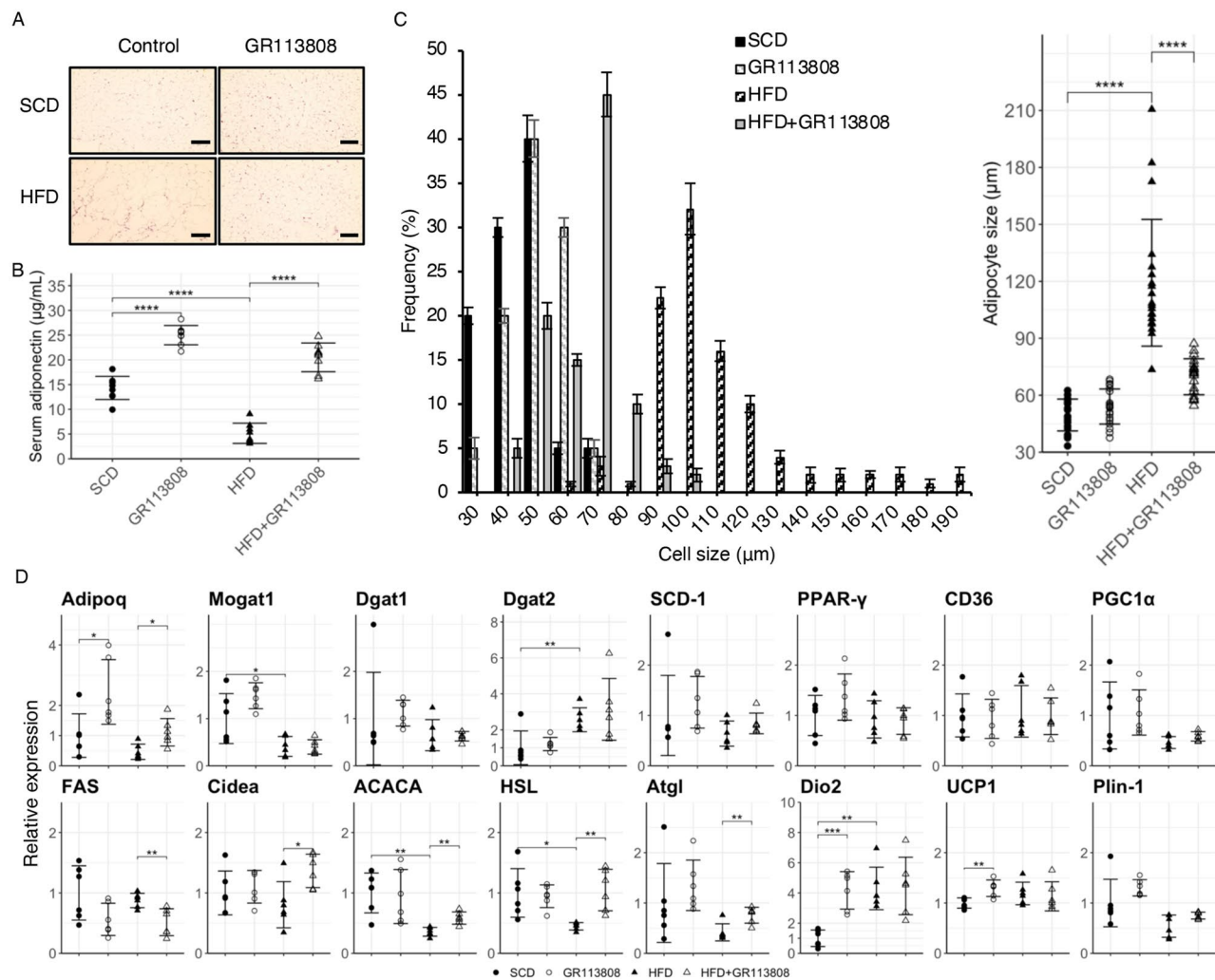


Fig. 4 GR113808 reduces the size of adipocytes in inguinal WAT but increases adiponectin production. **(A)** Histologic section of inguinal WAT (scale bar: 100 μm). **(B)** Serum adiponectin was measured using ELISA kits ($n=8-9$). **(C)** Adipocyte size distribution and mean adipocyte size ($n=20$). **(D)** Relative mRNA levels of genes related to lipogenesis (*Mogat1*, *Dgat1*, *Dgat2*, *ACACA*, *FAS*, *SCD-1*, and *PPAR-γ*), fatty acid uptake (*CD36*), thermogenesis (*Dio2*, *PGC1α*, *UCP1*, and *Cidea*), and lipolysis (*HSL* and *Atgl*) in the WAT of mice injected with GR113808 ($n=6$). A student's *t*-test was performed. Error bars on plots represent standard deviation (SD); * $p < 0.05$, ** $p < 0.01$, *** $p < 0.001$, **** $p < 0.0001$. Abbreviations: *ACACA* acetyl-CoA carboxylase alpha, *Adipoq* adiponectin, *Atgl* adipose triglyceride lipase, *CD36* cluster of differentiation 36, *Cidea* cell death-inducing DFFA-like effector A, *Dgat* diacylglycerol O-acyltransferase, *Dio2* iodothyronine deiodinase 2, *ELISA* enzyme-linked immunosorbent assay, *FAS* fatty acid synthase, *HFD* high-fat diet, *HSL* hormone-sensitive lipase, *Mogat1* monoacylglycerol O-acyltransferase 1, *PGC1α* peroxisome proliferator-activated receptor gamma coactivator 1-alpha, *PLIN1* perilipin 1, *PPAR* peroxisome proliferator-activated receptor, *SCD* standard chow diet, *SCD-1* stearoyl-CoA desaturase 1, *UCP* uncoupling protein, *WAT* white adipose tissue

iodothyronine deiodinase 2 (*Dio2*) expression in WAT of SCD-fed mice (Fig. 4D).

GR113808 reduced HFD-induced inflammation and inflammasome formation

Because adiponectin has anti-inflammatory and anti-atherogenic properties [17, 18], we examined inflammation in the serum, liver, and WAT. First, we examined serum inflammatory cytokine levels. GR113808 reduced the levels of inflammatory cytokines, such as TNF- α , IL-1 β , and IL-6 (Fig. 5A). Furthermore, the expression of genes related to inflammasome complex formation (NLRP3,

ASC, caspase-1, and IL-1 β) and inflammatory cytokine production (TNF- α , IL-1 β , IL-6, and monocyte chemoattractant protein-1 [MCP-1]) in the liver and adipose tissues was reduced upon GR113808 injection (Fig. 5B–E). HFD feeding increased the level of adhesion G-protein-coupled receptor E1 (F4/80), a macrophage marker [19], and GR113808 reduced F4/80 levels in the WAT (Fig. 5E).

Effects of HTR4 downregulation in Hep3B and 3T3-L1 cells

To further examine whether downregulation of HTR4 affects the PPAR- γ and SREBP-1 pathways, as well as inflammasome complex formation, we downregulated

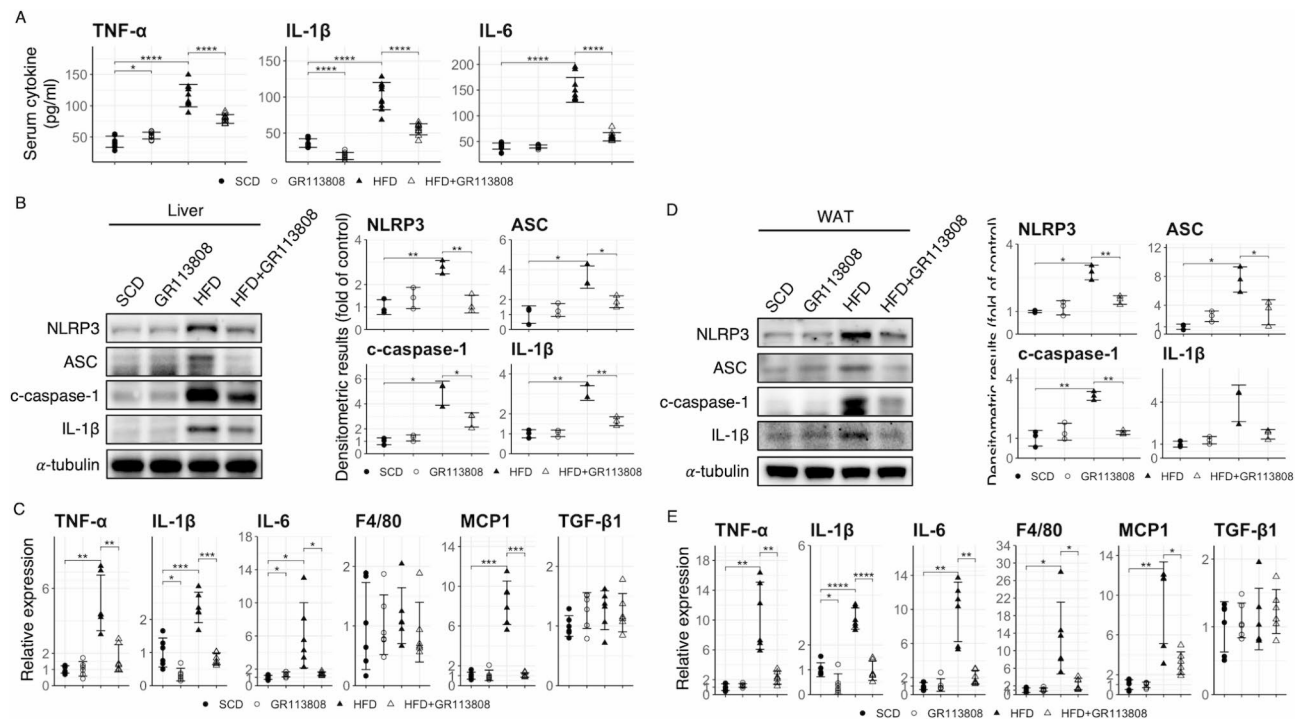


Fig. 5 GR113808 decreases inflammation in the serum and hepatic and adipose tissues. **(A)** Serum TNF- α , IL-1 β , and IL-6 levels measured using ELISA kits ($n = 10$). **(B)** Representative western blots (*left*) and densitometric analysis (*right*) of inflammasome complex formation in the liver ($n = 3$). **(C)** Relative mRNA levels of inflammation-related genes in the liver ($n = 6$). **(D)** Representative western blots (*left*) and densitometric analysis (*right*) of inflammasome complex formation in the WAT ($n = 3$). **(E)** Relative mRNA levels of inflammation-related genes in the WAT ($n = 6$). A student's *t*-test was performed. Error bars on plots represent standard deviation (SD); * $p < 0.05$, ** $p < 0.01$, *** $p < 0.001$, **** $p < 0.0001$. Abbreviations ASC apoptosis-associated speck-like protein containing a caspase-recruitment domain, *c-caspase-1* cleaved caspase-1, ELISA enzyme-linked immunosorbent assay, *F4/80* (*ADGRE1*) adhesion G-protein-coupled receptor E1, *HFD* high-fat diet, *IL* interleukin, *MCP-1* monocyte chemoattractant protein-1, *NLRP3* NOD-like receptor family pyrin domain containing 3, *SCD* standard chow diet, *TNF* tumor necrosis factor, *WAT* white adipose tissue

HTR4 using siRNA in Hep3B cells and then treated them with palmitate to mimic an HFD. Palmitate treatment (200 μ M) increased the expression of the mature form of SREBP-1 and its targets (FAS and SCD-1) (Fig. 6A). Additionally, palmitate treatment upregulated the expression of PPAR- γ , CD36, and proteins associated with inflammasome complex formation (NLRP3, ASC, caspase-1, and IL-1 β). This treatment also led to activation of the ER stress pathway, as evidenced by increased PERK and eIF2 α phosphorylation. Notably, HTR4 downregulation with siHTR4 suppressed the overexpression of genes involved in lipogenesis (SREBP-1, FAS, SCD-1), fatty acid uptake (PPAR- γ , CD36), the inflammasome complex (NLRP3, caspase-1, IL-1 β), and the ER stress pathway (PERK, eIF2 α) (Fig. 6A). Furthermore, HTR4 downregulation attenuated palmitate-induced TNF- α , IL-1 β , and IL-6 formation (Fig. 6B). To further examine the role of HTR4 in adipocytes, we conducted experiments wherein HTR4 was downregulated, followed by treatment with 200 μ M palmitate to induce inflammation in 3T3-L1 cells. The results indicated that HTR4 downregulation in 3T3-L1 cells mitigated palmitate-induced ER stress,

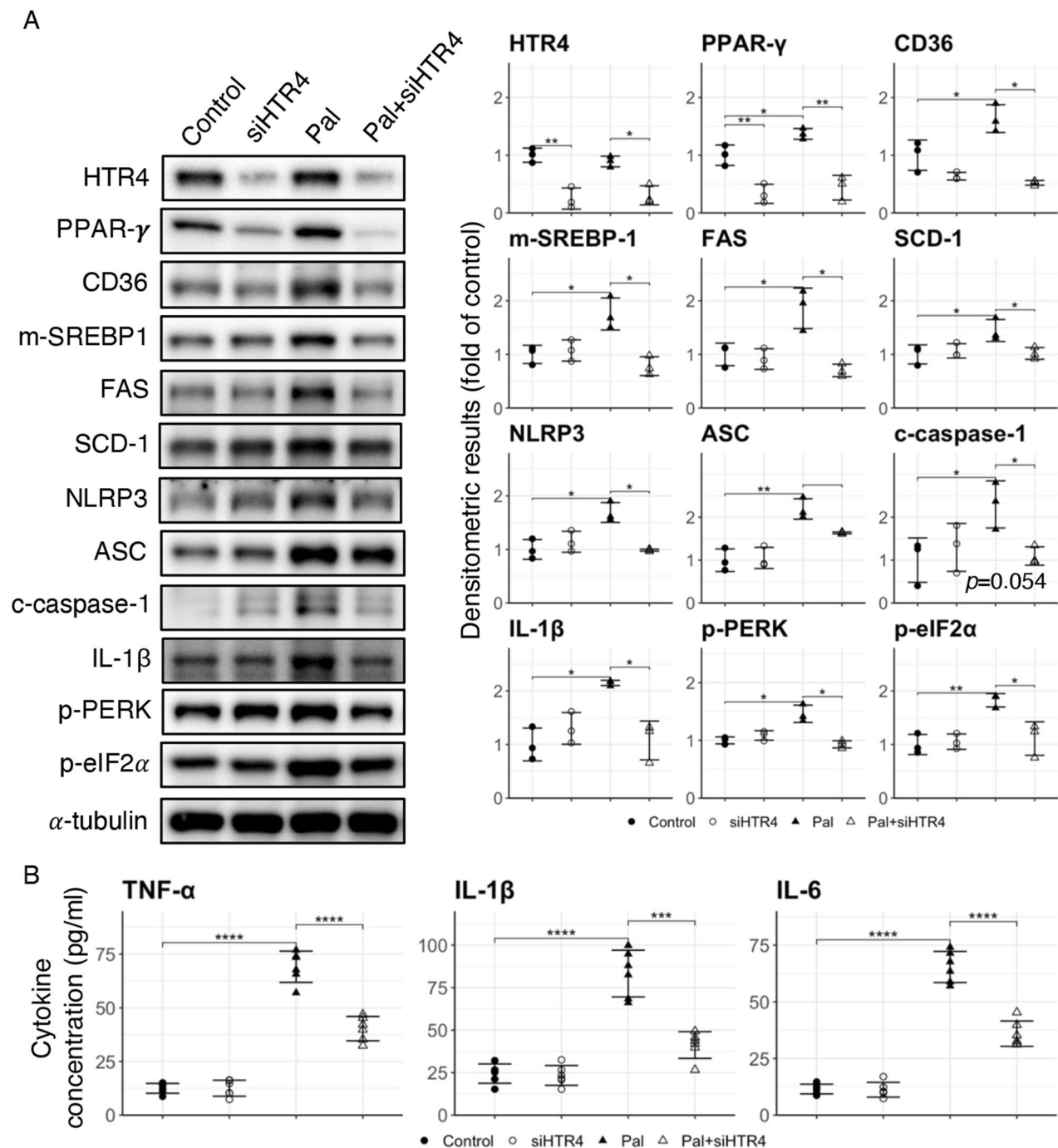
inflammasome complex formation, and inflammatory cytokine production (Fig. 7A and B).

Insulin resistance induced by palmitate treatment was improved by HTR4 downregulation in Hep3B cells but not in 3T3-L1 cells

To explore whether downregulation of HTR4 affects insulin resistance, we applied 200 μ M palmitate, followed by additional treatment with insulin for 2 or 5 min. Palmitate treatment decreased Akt phosphorylation in both Hep3B and 3T3-L1 cells (Fig. 8A and B), thus it induced insulin resistance. HTR4 downregulation recovered Akt phosphorylation in Hep3B cells but not in 3T3-L1 cells (Fig. 8A and B); therefore, HTR4 plays an important role in insulin resistance in the liver.

Discussion

In this study, we aimed to investigate the role of GR113808, a known HTR4 antagonist, during HFD feeding to understand its potential implications in NAFLD. Given the already high prevalence of NAFLD, which is expected to rise due to the increasing global obesity rate, there is a pressing need for effective treatments.



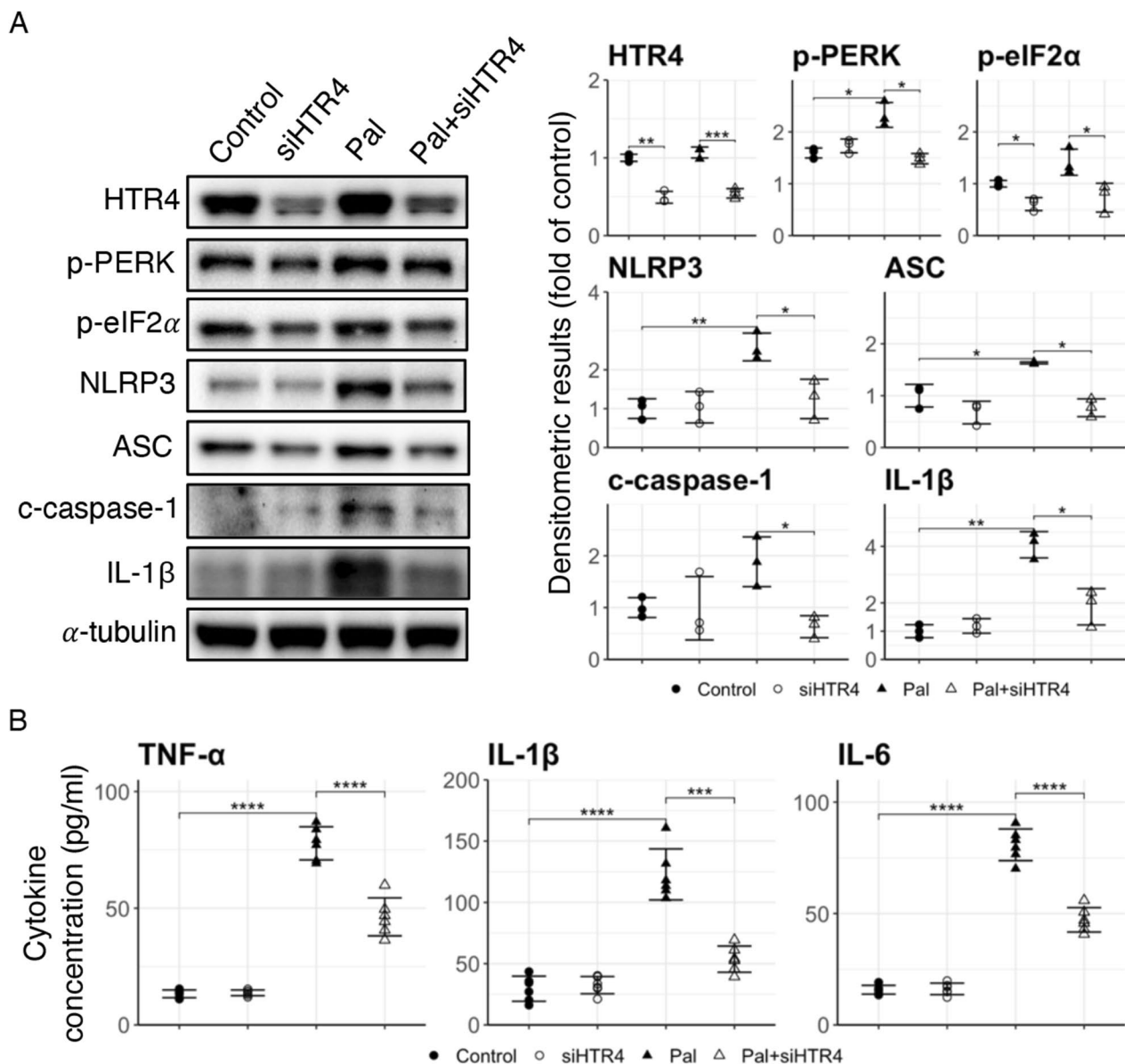


Fig. 7 HTR4 downregulation in 3T3-L1 cells prevents palmitate-induced inflammasome complex formation. **(A)** Representative western blots (*left*) and densitometric analysis (*right*) of the indicated protein ($n = 3$) and **(B)** levels of TNF- α , IL-1 β , and IL-6 in 3T3-L1 cell culture medium measured using an ELISA kit after 200 μ M palmitate treatment in HTR4-downregulated 3T3-L1 cells ($n = 6$). A student's *t*-test was performed. Error bars on plots represent standard deviation (SD); * $p < 0.05$, ** $p < 0.01$, *** $p < 0.001$. Abbreviations ASC apoptosis-associated speck-like protein containing a caspase-recruitment domain, *c-caspase-1* cleaved caspase-1, *eIF2 α* eukaryotic translation initiation factor 2 α , *ELISA* enzyme-linked immunosorbent assay, *HTR* serotonin receptor, *IL* interleukin, *NLRP3* NOD-like receptor family pyrin domain containing 3, *PERK* protein kinase R-like endoplasmic reticulum kinase, *TNF* tumor necrosis factor

Currently, numerous new drugs are being developed to address obesity and its associated conditions, including NAFLD, with some showing promise in ameliorating NAFLD in obese individuals [20].

In our study, we introduced a selective HTR4 antagonist, GR113808, as a potential drug candidate for NAFLD treatment. Our findings indicated that this antagonist suppressed fatty liver formation and prevented obesity and hyperglycemia in mice subjected to HFD feeding.

5-HT has previously been recognized for its role in regulating energy balance and glucose homeostasis through both central and peripheral mechanisms [5]. However, to the best of our knowledge, our study represents the first report on the effects of an HTR4 antagonist on obesity and hepatic fat accumulation.

Remarkably, despite HFD feeding leading to decreased HTR4 expression in hepatic and adipose tissues, our study found that injection of the HTR4 antagonist

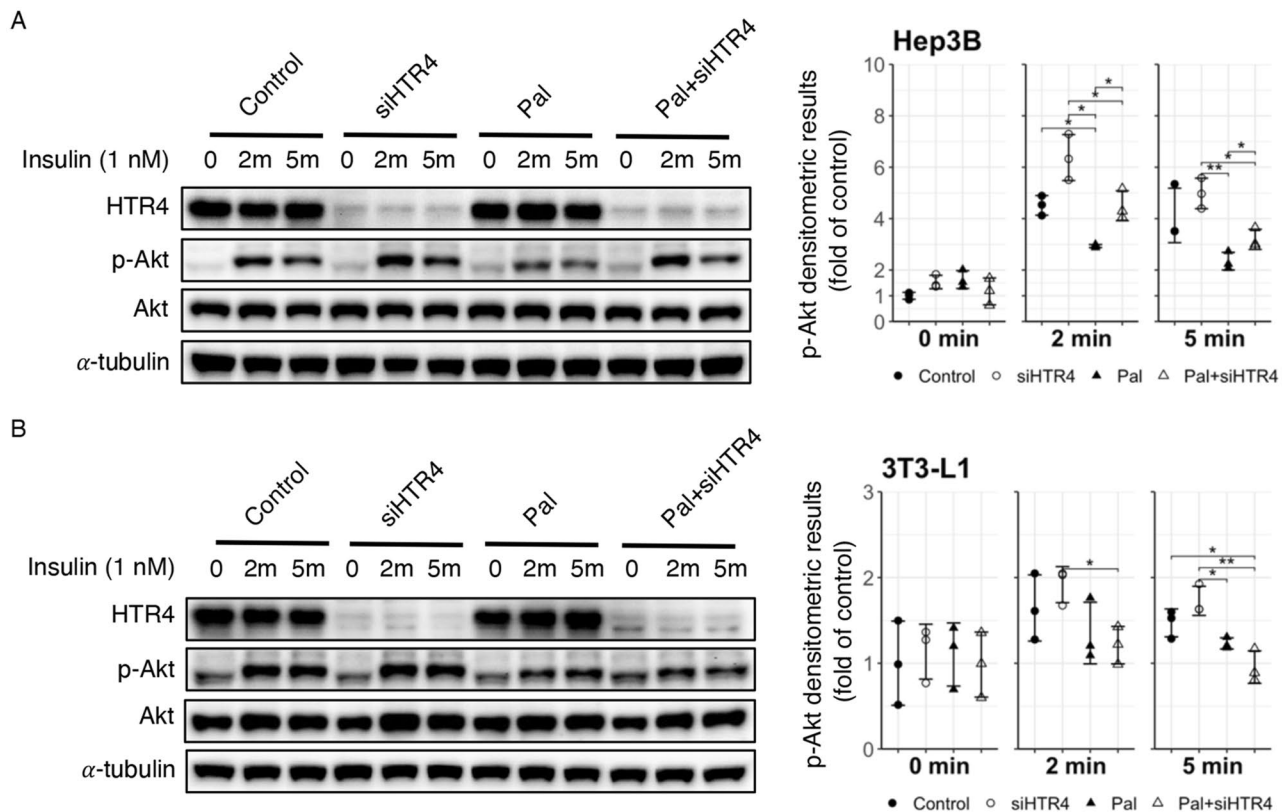


Fig. 8 HTR4 downregulation improves palmitate-induced insulin resistance in Hep3B cells, but not in 3T3-L1 cells. Representative western blots (left) and densitometric analysis (right) of the indicated protein upon insulin (1 nM) treatment after 200 μ M palmitate treatment in HTR4-downregulated Hep3B (A) and 3T3-L1 cells (B) ($n=3$) are shown. A student's *t*-test was performed. Error bars on plots represent standard deviation (SD); * $p < 0.05$, ** $p < 0.01$. All experiments were performed in triplicate. *Abbreviations* Akt protein kinase B, HTR serotonin receptor

GR113808 improved insulin resistance and fatty liver formation in HFD-fed mice. GR113808 administration resulted in reduced body, liver, and adipose tissue weights in both the SCD- and HFD-fed groups. The weight-suppressing effects of GR113808 are likely mediated through peripheral mechanisms, including the suppression of lipogenesis and fatty acid uptake. Two key transcription factors involved in these processes are SREBP-1 and PPAR- γ . SREBP-1 regulates the expression of lipogenesis genes such as FAS and SCD-1 [15, 21], while PPAR- γ regulates CD36, fat-specific protein 27 (FSP27), Mogat1, and lipoprotein lipase (LPL) [16], which are all crucial for lipogenesis and lipid uptake. Both SREBP-1c and PPAR- γ are overexpressed in individuals with obesity and NAFLD [22], and their dysregulation contributes to the pathogenesis of these conditions. PPAR- γ heterozygotic (+/-) mice are protected from HFD-induced obesity and insulin resistance [9]. Moreover, SREBP-1c mRNA and mature protein levels are elevated in ob/ob mouse livers [21], and SREBP-1 overexpression leads to fatty liver formation [23]. Studies in animal models have shown that manipulation of these factors can impact obesity and insulin resistance.

GR113808 treatment reduced the expression of SREBP-1c, FAS, SCD-1, PPAR- γ , CD36, Mogat1, and FABP1, all of which are involved in lipogenesis and fatty acid uptake. Moreover, downregulation of HTR4 mimicked the effects of GR113808 treatment, suggesting that HTR4 plays a crucial role in these processes. Consequently, downregulation of HTR4 and treatment with GR113808 reduced fatty liver formation by modulating the SREBP-1c and PPAR- γ pathways and decreasing ER stress, which affects SREBP-1 and FAS expression [24]. It is unclear how the HTR4 antagonist GR113808 modulates PPAR- γ and SREBP-1, but this effect could be influenced by various factors, such as nutritional status, ER stress or adiponectin levels. Insulin can increase the expression of PPAR- γ [25] and high energy states, such as high glucose levels, also stimulate SREBP-1 transcription via mTOR signaling [26]. mTOR and AMPK are complementary energy sensors that regulate the expression of SREBP-1 in response to energy status [26, 27]. ER stress also upregulates SREBP-1 expression and SREBP-1 cleavage [24, 28], while adiponectin suppresses SREBP-1 expression [29]. Thus, a high energy state and ER stress may increase the expression of PPAR- γ and SREBP-1, leading to increased

lipogenesis and lipid uptake. GR113808 may inhibit the expression of PPAR- γ and SREBP-1 by reducing ER stress, lowering energy state, and increased adiponectin production.

Inflammation can be triggered by various inflammatory stimuli, leading to increased production of inflammatory cytokines such as TNF- α , IL-1 β , IL-6, and MCP-1 [30, 31]. Fatty acid overflow, a consequence of conditions such as obesity, contributes to chronic low-grade inflammation [30]. Specifically, overflow of saturated fatty acids such as palmitate and stearate exacerbates lipotoxicity, which in turn induces hepatotoxicity and pancreatic β -cell death in metabolic diseases such as diabetes. Lipotoxicity manifests through mechanisms including reactive oxygen species damage, inflammation, cell death, and mitochondrial dysfunction [30, 32]. Notably, GR113808 injection led to increased serum adiponectin levels and adiponectin mRNA expression in adipose tissue. Adiponectin is known for its anti-inflammatory and anti-atherogenic properties, serving as an insulin-sensitizing adipokine that aids in maintaining whole-body energy homeostasis [17]. Decreased adiponectin levels are observed in obesity, with a similar reduction noted in patients with NAFLD [33, 34]. Adiponectin ameliorates insulin resistance [35], and its supplementation has shown promise in alleviating fatty liver disease and improving insulin resistance, acting as an anti-inflammatory mediator [18, 36]. The elevation of adiponectin levels following GR113808 injection suggests a potential mechanism for reducing HFD-induced inflammation, fatty liver formation, and insulin resistance. Indeed, GR113808 administration resulted in reduced serum levels of inflammatory cytokines (TNF- α , IL-1 β , and IL-6) and decreased expression of these cytokines, as well as MCP-1; its administration also reduced inflammasome complex formation in hepatic and adipose tissues. Additionally, GR113808 recovered insulin resistance after HFD feeding. HTR4 downregulation mirrored these effects, suggesting the involvement of HTR4 in inflammation- and insulin-related pathways. Altogether, the secretion of adiponectin and downregulation of HTR4 contributed to the mitigation of inflammation, inflammasome complex formation, and insulin resistance.

Some HTR subtypes are also associated with NAFLD. In a previous study, HTR2a expression was increased in HFD-fed mouse livers, and HTR2a liver-specific knockout mice were protected from fatty liver formation [12]. Additionally, HTR3 antagonists reduced fatty liver formation, liver inflammation, and liver cell necrosis in ob/ob mice [37]. Furthermore, modulation of 5-HT in the gut–liver neural axis decreased fatty liver formation and liver inflammation [38], and HTR2a antagonists have shown therapeutic potential for the treatment of NAFLD induced by diet [39]. In this study, even though HTR4

expression in the liver was low (Table S2), we showed that HTR4 antagonists have similar protective effects against fatty liver formation and obesity. However, we are uncertain whether the findings can be applied to humans in the same manner. Further investigation into the role of HTR4 in obesity, fatty liver, inflammation, and insulin resistance in humans is needed.

Because 5-HT is synthesized in neurons and acts as a neurotransmitter, it can modulate the gut–liver neural axis, which might occur through HTR2a, HTR3, and HTR4. Therefore, inhibition of these receptors may be an effective strategy for treating obesity and fatty liver formation.

Our study demonstrated that GR113808 improved NAFLD through inhibitory effects on lipogenesis, fatty acid uptake, and inflammation. Although GR113808 has been shown to antagonize HTR4, there is a possibility of some degree of concurrent action on other HTR subtypes. However, GR113808 did not affect HTR expression in Hep3B and 3T3-L1 cells, indicating that it does not impact HTR expression (Fig. S2). Reproduction of the results in HTR4 knockout mice is necessary to confirm whether the effects of GR113808 are solely mediated through antagonism of HTR4. The absence of data from knockout mice is a limitation of our study. Nevertheless, transfection of siHTR4 into Hep3B and 3T3-L1 cells, resulting in the suppression of HTR4 at the cellular level, provides evidence that inhibiting HTR4 can improve NAFLD-related metabolic processes.

Conclusions

Injection of the HTR4 antagonist GR113808 suppressed obesity and fatty liver formation and improved inflammation in the liver and adipose tissue. Additionally, HTR4 downregulation improved hepatic insulin resistance. Thus, HTR4 may be an attractive target for treatment of NAFLD associated with obesity and type 2 diabetes.

Abbreviations

5-HT	5-hydroxytryptamine, serotonin
ACACA	Acetyl-CoA carboxylase alpha
Acox1	Acyl-CoA oxidase 1
Adipoq	Adiponectin
Agpat1	1-acylglycerol-3-phosphate O-acyltransferase 1
Akt	Protein kinase B
ASC	Apoptosis-associated speck-like protein containing a caspase-recruitment domain
Atgl	Adipose triglyceride lipase
CD36	Cluster of differentiation 36
Cidea	Cell death-inducing DFFA-like effector A
Cpt1a	Carnitine palmitoyl transferase 1a
Dgat	Diacylglycerol O-acyltransferase
Dio2	Iodothyronine deiodinase 2
eIF2 α	Eukaryotic translation initiation factor 2 α
ER	Endoplasmic reticulum
FABP	Fatty acid binding protein
FAS	Fatty acid synthase
FATP5	Fatty acid transport protein 5
F4/80	Adhesion G-protein-coupled receptor E1

FSP27	Fat-specific protein 27
GTT	Glucose tolerance test
HDL	High-density lipoprotein
HFD	High-fat diet
HRP	Horseradish peroxidase
HSL	Hormone-sensitive lipase
HTR	5-hydroxytryptamine receptor
IL	Interleukin
LDL	Low-density lipoprotein
LPL	Lipoprotein lipase
MCP-1	Monocyte chemoattractant protein-1
Mogat1	Monoacylglycerol O-acyltransferase 1
NAFLD	Nonalcoholic fatty liver disease
NLRP3	NOD-like receptor family pyrin domain containing 3
PERK	Protein kinase R-like endoplasmic reticulum kinase
PGC1 α	Peroxisome proliferator-activated receptor gamma coactivator 1-alpha
PLIN1	Perilipin 1
PPAR	Peroxisome proliferator-activated receptor
SCD	Standard chow diet
SCD-1	Stearoyl-CoA desaturase-1
SREBP	Sterol regulatory element-binding protein
TNF	Tumor necrosis factor
UCP	Uncoupling protein
WAT	White adipose tissue

Supplementary Information

The online version contains supplementary material available at <https://doi.org/10.1186/s40360-024-00800-3>.

Supplementary Material 1

Acknowledgements

Not applicable.

Author contributions

M.H.K.: Methodology, Investigation, Resources, Data curation. S.K.: Investigation, Resources. W.P.: Conceptualization, Methodology, Validation, Formal analysis, Data curation, Writing—original draft preparation, Visualization, Supervision, Project administration. D.H.L.: Writing—review and editing, Funding acquisition. K.K.: Conceptualization, Writing—review and editing, Supervision, Project administration, Funding acquisition. All authors read and approved the final manuscript.

Funding

This work was supported by a National Research Foundation of Korea grant funded by the Ministry of Education, Science and Technology, Korea [Grant number, NRF-2021R1F1A1057106]; a grant from the Korea Health Technology Research & Development Project through the Korea Health Industry Development Institute, funded by the Ministry of Health & Welfare, Korea [Grant number, HI14C1135]; and Ildong Pharmaceutical Company, Korea [Grant number, Ildong-LCDI-2018-0143]. No funder has role in in the conceptualization, design, data collection, analysis, decision to publish, or preparation of the manuscript.

Data availability

No datasets were generated or analysed during the current study.

Declarations

Ethics approval and consent to participate

All animal experiments were carried out in accordance with the Guide for the Care and Use of Laboratory Animals as adopted and promulgated by the U.S. National Institutes of Health and were approved by the Animal Ethics Committee of the LeeGilYa Cancer and Diabetes Institute (LCDI-2021-0079).

Consent for publication

Not applicable.

Competing interests

The authors declare no competing interests.

Author details

¹Department of Biochemistry, Ewha Womans University College of Medicine, Seoul 07084, Republic of Korea

²Department of Biochemistry, Gachon University College of Medicine, Incheon 21565, Republic of Korea

³Department of Biochemistry, Chung-Ang University College of Medicine, Seoul 06974, Republic of Korea

⁴Department of Internal Medicine, Gachon University Gil Medical Center, Gachon University College of Medicine, Incheon 21565, Republic of Korea

⁵Department of Family Medicine, Gachon University Gil Medical Center, Gachon University College of Medicine, Incheon 21565, Republic of Korea

Received: 31 May 2024 / Accepted: 7 October 2024

Published online: 11 October 2024

References

- Powell EE, Wong VW-S, Rinella M. Non-alcoholic fatty liver disease. *Lancet*. 2021;397(10290):2212–24.
- Sumida Y, Yoneda M. Current and future pharmacological therapies for NAFLD/NASH. *J Gastroenterol*. 2018;53(3):362–76.
- European Association for the Study of the Liver, European Association for the Study of Diabetes, European Association for the Study of Obesity. EASL-EASD-EASO clinical practice guidelines for the management of non-alcoholic fatty liver disease. *J Hepatol*. 2016;64(6):1388–402.
- El-Merahbi R, Löffler M, Mayer A, Sumara G. The roles of peripheral serotonin in metabolic homeostasis. *FEBS Lett*. 2015;589(15):1728–34.
- Lam DD, Heisler LK. Serotonin and energy balance: molecular mechanisms and implications for type 2 diabetes. *Expert Rev Mol Med*. 2007;9(5):1–24.
- Paulmann N, Grohmann M, Voigt J-P, Bert B, Vowinckel J, Bader M, et al. Intracellular serotonin modulates insulin secretion from pancreatic β -cells by protein serotonylation. *PLoS Biol*. 2009;7(10):e1000229.
- Lesurtel M, Graf R, Aleil B, Walther DJ, Tian Y, Jochum W, et al. Platelet-derived serotonin mediates liver regeneration. *Science*. 2006;312(5770):104–7.
- Wu H, Denna TH, Storkersen JN, Gerriets VA. Beyond a neurotransmitter: the role of serotonin in inflammation and immunity. *Pharmacol Res*. 2019;140:100–14.
- Kadowaki T, Hara K, Yamauchi T, Terauchi Y, Tobe K, Nagai R. Molecular mechanism of insulin resistance and obesity. *Exp Biol Med (Maywood)*. 2003;228(10):1111–17.
- Wu S, Wang X, Xing W, Li F, Liang M, Li K, et al. An update on animal models of liver fibrosis. *Front Med (Lausanne)*. 2023;10:1160053.
- Pedro PF, Tsakmaki A, Bewick GA. The glucose tolerance test in mice. *Methods Mol Biol*. 2020;2128:207–16.
- Choi W, Namkung J, Hwang I, Kim H, Lim A, Park HJ, et al. Serotonin signals through a gut-liver axis to regulate hepatic steatosis. *Nat Commun*. 2018;9(1):4824.
- Moody CM, Makowska JJ, Weary DM. Testing three measures of mouse insensibility following induction with isoflurane or carbon dioxide gas for a more humane euthanasia. *Appl Anim Behav Sci*. 2015;163:183–87.
- Livak KJ, Schmittgen TD. Analysis of relative gene expression data using real-time quantitative PCR and the 2(-delta delta C(T)) method. *Methods*. 2001;25(4):402–8.
- Postic C, Girard J. Contribution of de novo fatty acid synthesis to hepatic steatosis and insulin resistance: lessons from genetically engineered mice. *J Clin Invest*. 2008;118(3):829–38.
- Lee YK, Park JE, Lee M, Hardwick JP. Hepatic lipid homeostasis by peroxisome proliferator-activated receptor gamma 2. *Liver Res*. 2018;2(4):209–15.
- Lee B, Shao J. Adiponectin and energy homeostasis. *Rev Endocr Metab Disord*. 2014;15(2):149–56.
- Huang H, Park PH, McMullen MR, Nagy LE. Mechanisms for the anti-inflammatory effects of adiponectin in macrophages. *J Gastroenterol Hepatol*. 2008;23(Suppl 1):S50–3.
- Austyn JM, Gordon S. F4/80, a monoclonal antibody directed specifically against the mouse macrophage. *Eur J Immunol*. 1981;11(10):805–15.
- Newsome PN, Buchholtz K, Cusi K, Linder M, Okanou T, Ratziu V, et al. A placebo-controlled trial of subcutaneous semaglutide in nonalcoholic steatohepatitis. *N Engl J Med*. 2021;384(12):1113–24.

21. Shimomura I, Bashmakov Y, Horton JD. Increased levels of nuclear SREBP-1c associated with fatty livers in two mouse models of diabetes mellitus. *J Biol Chem*. 1999;274(42):30028–32.
22. Pettinelli P, Videla LA. Up-regulation of PPAR-gamma mRNA expression in the liver of obese patients: an additional reinforcing lipogenic mechanism to SREBP-1c induction. *J Clin Endocrinol Metab*. 2011;96(5):1424–30.
23. Shimano H, Horton JD, Shimomura I, Hammer RE, Brown MS, Goldstein JL. Isoform 1c of sterol regulatory element binding protein is less active than isoform 1a in livers of transgenic mice and in cultured cells. *J Clin Invest*. 1997;99(5):846–54.
24. Fang DL, Wan Y, Shen W, Cao J, Sun ZX, Yu HH, et al. Endoplasmic reticulum stress leads to lipid accumulation through upregulation of SREBP-1c in normal hepatic and hepatoma cells. *Mol Cell Biochem*. 2013;381(1–2):127–37.
25. Rieusset J, Andreelli F, Auboeuf D, Roques M, Vallier P, Riou JP, et al. Insulin acutely regulates the expression of the peroxisome proliferator-activated receptor-gamma in human adipocytes. *Diabetes*. 1999;48(4):699–705.
26. Peterson TR, Sengupta SS, Harris TE, Carmack AE, Kang SA, Balderas E, et al. mTOR complex 1 regulates lipin 1 localization to control the SREBP pathway. *Cell*. 2011;146(3):408–20.
27. Jung EJ, Kwon SW, Jung BH, Oh SH, Lee BH. Role of the AMPK/SREBP-1 pathway in the development of orotic acid-induced fatty liver. *J Lipid Res*. 2011;52(9):1617–25.
28. Kim YR, Lee EJ, Shin KO, Kim MH, Pewzner-Jung Y, Lee YM, et al. Hepatic triglyceride accumulation via endoplasmic reticulum stress-induced SREBP-1 activation is regulated by ceramide synthases. *Exp Mol Med*. 2019;51(11):1–16.
29. Awazawa M, Ueki K, Inabe K, Yamauchi T, Kaneko K, Okazaki Y, et al. Adiponectin suppresses hepatic SREBP1c expression in an AdipoR1/LKB1/AMPK dependent pathway. *Biochem Biophys Res Commun*. 2009;382(1):51–56.
30. Pereira SS, Alvarez-Leite JI. Low-grade inflammation, obesity, and diabetes. *Curr Obes Rep*. 2014;3(4):422–31.
31. Shaker ME. The contribution of sterile inflammation to the fatty liver disease and the potential therapies. *Biomed Pharmacother*. 2022;148:112789.
32. Mansouri A, Gattolliat CH, Asselah T. Mitochondrial dysfunction and signaling in chronic liver diseases. *Gastroenterology*. 2018;155(3):629–47.
33. Hu E, Liang P, Spiegelman BM. AdipoQ is a novel adipose-specific gene dysregulated in obesity. *J Biol Chem*. 1996;271(18):10697–703.
34. Pagano C, Soardo G, Esposito W, Fallo F, Basan L, Donnini D, et al. Plasma adiponectin is decreased in nonalcoholic fatty liver disease. *Eur J Endocrinol*. 2005;152(1):113–18.
35. Kadowaki T, Yamauchi T, Kubota N, Hara K, Ueki K, Tobe K. Adiponectin and adiponectin receptors in insulin resistance, diabetes, and the metabolic syndrome. *J Clin Invest*. 2006;116(7):1784–92.
36. Xu A, Wang Y, Keshaw H, Xu LY, Lam KS, Cooper GJ. The fat-derived hormone adiponectin alleviates alcoholic and nonalcoholic fatty liver diseases in mice. *J Clin Invest*. 2003;112(1):91–100.
37. Haub S, Ritze Y, Ladel I, Saum K, Hubert A, Spruss A, et al. Serotonin receptor type 3 antagonists improve obesity-associated fatty liver disease in mice. *J Pharmacol Exp Ther*. 2011;339(3):790–98.
38. Ko M, Kamimura K, Owaki T, Nagoya T, Sakai N, Nagayama I, et al. Modulation of serotonin in the gut-liver neural axis ameliorates the fatty and fibrotic changes in non-alcoholic fatty liver. *Dis Model Mech*. 2021;14(3):dmm048922.
39. Owaki T, Kamimura K, Ko M, Nagayama I, Nagoya T, Shibata O, et al. Involvement of the liver-gut peripheral neural axis in nonalcoholic fatty liver disease pathologies via hepatic HTR2A. *Dis Model Mech*. 2022;15(7):dmm049612.

Publisher's Note

Springer Nature remains neutral with regard to jurisdictional claims in published maps and institutional affiliations.